Journal of Constructional Steel Research 236 (2026) 109994

Contents lists available at ScienceDirect

Journal of Constructional Steel Research

journal homepage: www.elsevier.com/locate/jcsr

Review

Design method for transverse load resistance of web-posts in cellular beams

Konstantinos Daniel Tsavdaridis [a,*], Dan-Adrian Corfar [a], R. Mark Lawson [a,b]

[a] Department of Engineering, School of Science & Technology, City, University of London, EC1V 0HB London, UK
[b] The Steel Construction Institute, Unit 2, The E Centre, Bracknell RG12 1NF, UK

ARTICLE INFO

Keywords:
Cellular beams
Finite element analysis
Transverse loading
Plate buckling
Web-post buckling

ABSTRACT

The effect of transverse loads on the buckling resistance of the web-post between circular openings is assessed by finite element (FE) models that are calibrated against the results of a test on a cellular beam with transverse loads applied above two adjacent openings. The test failure load of the web-post was 250 kN of which 96 kN is attributed to web-post buckling and the rest to the transfer of load by local bending of the web-flange T-sections. The FE modelling showed that buckling of the web-post subject to transverse load can be predicted using the method of BS EN 1993-1-5 with a buckling coefficient that is a function of the edge spacing of the openings to the beam web depth. The FE results considered a range of geometric parameters and two steel strengths. It was found that the stresses across the web-post are non-uniform and a formula for the effective web-post width is presented. With this modification, the ratio of the predicted web-post buckling resistance to the isolated web-post buckling load obtained from the FEA was in the range of 0.80 to 0.99. The load transfer by local bending of the top Tee was determined from the elastic bending resistance of the Tee and the ratio to the failure load from the FEA was conservatively in the range of 0.62 to 0.77. Based on this study, a design formula for the web-post buckling resistance of cellular beams to transverse loads is derived.

1. Introduction

Cellular beams are widely used in buildings due to their high strength-to-weight ratio and provision of multiple circular openings for services distribution. However, their performance under transverse loads applied to the web-post has not been previously investigated, despite being an important practical design case, such as when heavily loaded purlins or secondary beams are connected to the beam top flange or to the web-post between the circular openings. Transverse loads interact with the web-post forces arising from shear transfer, potentially leading to a critical failure mode. Currently, there are no specific design rules for web bearing and buckling in cellular beams under transverse loading in BS EN 1993-1-5 [1] or on the general provisions for beams with large web openings in BS EN 1993-1-13 [2].

To address this gap, this study presents the first systematic evaluation of the web-post buckling resistance to transverse loads in cellular beams. In this study, the transverse loads were applied to the top flange of a cellular beam. A load test was conducted on a 560 mm deep cellular beam to assess the structural behaviour of the web-posts to transverse loads and to validate numerical models. Following this, a parametric finite element analysis (FEA) study was performed to investigate the influence of the web thickness, opening diameter, web-post width, and steel grade on the web-post buckling resistance and the controlling failure modes. Based on these findings, design rules are proposed within the framework of the plate buckling method in BS EN 1993-1-5 [1]. A comparison is made with the equivalent strut buckling method in BS EN 1993-1-1 [3], using buckling curve "c" and two different effective lengths. The accuracy of these design rules was assessed by comparing their predictions to the FEA results. Overall, this study aims to enhance the structural reliability of cellular beams and contribute to the development of improved design recommendations.

2. Design methods for web-post buckling under transverse loads

2.1. Background on web buckling and basis of Eurocode rules

The rules in BS EN 1993-1-5 for web yielding and buckling of beams subject to transverse loads were developed by Lagerqvist and Johansson [4]. This work built on the earlier contribution by Roberts [5], who had investigated the resistance of slender plate girders subjected to localised edge loading in the plane of the web.

The development of the design rules considered three typical

* Corresponding author.
E-mail address: Konstantinos.Tsavdaridis@city.ac.uk (K.D. Tsavdaridis).

https://doi.org/10.1016/j.jcsr.2025.109994
Received 9 June 2025; Received in revised form 25 August 2025; Accepted 16 September 2025
Available online 25 September 2025

transverse loading conditions: (1) load applied to the web through one flange, (2) load applied in opposite directions to both flanges, and (3) load applied close to the free edge of the beam. The design approach was formulated as a function of the loaded length, considering both plastic bending of the top flange and the upper part of the web in bearing, as well as the slenderness of the web in buckling.

The buckling resistance of the web was calibrated to the results of 60 tests on welded and rolled beams. The results were used to validate FE models, taking account of the web and flange thickness, the loaded length, and the web depth-to-thickness ratio. Together with data from a global database, a total of 186 tests was considered in the development of the design procedure.

Based on this dataset, a simplified buckling curve was proposed for transverse loading. This curve differs in shape from the plate buckling curve used for shear and strut buckling, reflecting the distinct local behaviour of the web under concentrated transverse loads.

The relative slenderness of the web, $\bar{\lambda}$, is defined by Eq. (1):

$$\bar{\lambda} = \left(\frac{f_y}{\sigma_{cr}}\right)^{0.5} \tag{1}$$

Where f_y is the steel yield strength

And σ_{cr} is the critical buckling strength of the web, given by Eq. (2):

$$\sigma_{cr} = k_f \frac{\pi^2}{12(1-\nu^2)} E \left(\frac{t_w}{h_w}\right)^2 = 0.9 k_f E \left(\frac{t_w}{h_w}\right)^2 \tag{2}$$

Where k_f is the buckling coefficient of the web for this mode of failure,

E is Young's modulus,

t_w is the web thickness,

And h_w is the web panel depth between the flanges.

Combining Eqs. (1) and (2) leads to Eq. (3) for the relative slenderness of the web:

$$\bar{\lambda} = \frac{1}{28.4 k_f^{0.5} \varepsilon} \left(\frac{h_w}{t_w}\right) \tag{3}$$

Where $\varepsilon = \left(235/f_y\right)^{0.5}$.

The buckling curve for web buckling proposed by Lagerqvist and Johansson [4] was defined by Eq. (4), having a cut-off at $\chi = 1$ at a relative slenderness, $\bar{\lambda}$, of 0.5.

$$\chi = 0.06 + \frac{0.47}{\bar{\lambda}} \leq 1.0 \tag{4}$$

BS EN 1993-1-5 [1] simplifies this buckling curve – see next section. The study also considered the influence of the global bending moment on the results of the patch load tests. The interaction between transverse load and moment acting on the beam was captured by reducing the patch load resistance using Eq. (5):

$$\frac{F_{w,Ed}}{F_{w,Rd}} + 0.8 \frac{M_{Ed}}{M_{Rd}} \leq 1.4 \tag{5}$$

Where M_{Ed} is the applied moment at the load position,

M_{Rd} is the beam bending resistance,

$F_{w,Ed}$ is the applied transverse (patch) load.

And $F_{w,Rd}$ is the resistance of the web to transverse load.

Roberts and Shahabian [6] later extended the study of interaction effects to slender webs under combined shear and patch loading, proposing the interaction rule given by Eq. (6):

$$\frac{F_{w,Ed}}{F_{w,Rd}} + \left(\frac{V_{Ed}}{V_{b,Rd}}\right)^2 \leq 1.0 \tag{6}$$

- Where $\boldsymbol{V_{Ed}}$ is the applied shear force,

And $V_{b,Rd}$ is the buckling resistance of the web in shear.

2.2. Current Eurocode provisions

The design of beams with large web openings is presented in BS EN 1993-1-13 [2] and limits are also given on the minimum edge to edge spacing of openings. Web-post buckling for beams with circular and rectangular openings is analysed by treating the web-post as an equivalent strut using buckling curve 'a' to BS EN 1993-1-1 [3]. There are no specific provisions for transverse load for beams with web openings, except for local loads applied directly to the top flange of beams over long openings. Also for web buckling, BS EN 1993-1-1 [3] refers to BS EN 1993-1-5 [1] to determine the web bearing and buckling resistance of a beam subject to local transverse loads.

The design resistance to transverse forces applied to the web is given by Eq. (7):

$$F_{w,Rd} = \frac{f_{yw} L_{eff} t_w}{\gamma_{M1}} \tag{7}$$

Where $f_{y,w}$ is the yield strength of the web,

t_w is the web thickness,

L_{eff} is the effective length for resistance to transverse forces,

And $\gamma_{M1} = 1.0$ for this mode.

L_{eff} is dependent on the relative slenderness of the web and is determined from Eq. (8):

$$L_{eff} = \chi_F \ell_y \tag{8}$$

Where ℓ_y is the effective loaded length depending on the relative proportions of the flange and web given in BS EN 1993-1-5 [1].

Compared to the expression suggested by Lagerqvist and Johansson [4], the reduction factor due to web buckling, χ_F, is given in BS EN 1993-1-5 [1] by a simpler but slightly more conservative Eq. (9):

$$\chi_F = \frac{0.5}{\bar{\lambda}_F} \leq 1.0 \tag{9}$$

where $\bar{\lambda}_F$ is obtained from Eq. (10):

$$\bar{\lambda}_F = \left(\frac{\ell_y t_w f_y}{F_{cr}}\right)^{0.5} \tag{10}$$

where F_{cr} is the critical force for buckling of the web, which is equal to the buckling strength multiplied by $h_w t_w$ for a 45° load dispersion to mid-height of the web, and is determined by Eq. (11):

$$F_{cr} = 0.9 k_f E \frac{t_w^3}{h_w} \tag{11}$$

For the case of patch loading with widely spaced stiffeners, k_f is taken as 6, which implies that 2-way bending action of the web and some rotational stiffness of the flange occur below the load position.

For the case of loading near the edge of the beam, k_f is given in BS EN 1993-1-5 [1] by Eq. (12):

$$k_f = 2 + 6 \frac{(s_s + c)}{h_w} \leq 6 \tag{12}$$

Where c is the distance from the edge of the patch loading to the edge of the beam,

And s_s is the length of the patch load.

It follows that when $s_s + c > 2/3 h_w$, then the edge effect can be ignored.

2.3. Application of transverse loads in cellular beams

The case of a free edge on both sides of the patch load is not explicitly addressed in BS EN 1993-1-5 [1]. This study builds on that observation by proposing an adaptation of the plate buckling model, based on the idea that extending the single free edge condition to both edges being unrestrained — such as between adjacent openings — results in a

geometry representative of a web-post.

In the limit, the buckling coefficient tends to $k_f \approx 1$, which corresponds to an effective strut length of h_w assuming that the flanges offer little end fixity. A more accurate formula for the buckling coefficient, k_f, of a narrow web-post is considered in this paper.

For the case of web-post buckling, the critical buckling force may then be obtained by multiplying σ_{cr} with the web-post cross-sectional area as shown in Eq. (13):

$$F_{cr} = \sigma_{cr} s_o t_w \tag{13}$$

Where s_o is the width of the web-post at the centreline of the openings.

It is shown later that the stresses across wider and slender web-posts are non-uniform and so a modification to the effective web-post width is proposed. An alternative representation of the failure mechanism as an equivalent strut is also considered, using the representative strut buckling curve given in BS EN 1993-1-1 [3].

To assess the suitability of each approach, Fig. 1 presents a comparison between the reduction factors obtained from the plate buckling model and those from the strut buckling curve 'c', across a range of relative slenderness values. As shown, the difference in predicted resistance becomes more pronounced for more slender plates.

It should be noted that buckling curve 'a' is used in the BS EN 1993-1-13 [2] equivalent strut model for web-post buckling due to horizontal shear. The buckling resistance of the web-post using buckling curve 'a' correlates well with cellular beam tests in which the buckling mode has a point of zero deformation at the centreline of the web. Therefore, the imperfection parameter for the web is less than for the case of transverse loads, in which the web-post buckles over a longer length and the imperfection parameter is more accurately modelled using buckling curve 'c'.

3. Test on the web-post buckling resistance of a cellular beam to transverse loads

A load test was carried out on a cellular beam to determine the stability of the web-post subject to a compression force from two jack loads applied directly above the adjacent openings. The test arrangement is shown in Fig. 2 (a)-(c).

Although the ideal loading condition would have been a single concentrated force applied directly above the web-post, this was not feasible due to the presence of a lateral–torsional buckling restraint at mid-span, which would have interfered with jack placement. Instead, the most feasible alternative was to apply two loads above the adjacent openings. This arrangement allowed the desired web-post behaviour to be activated.

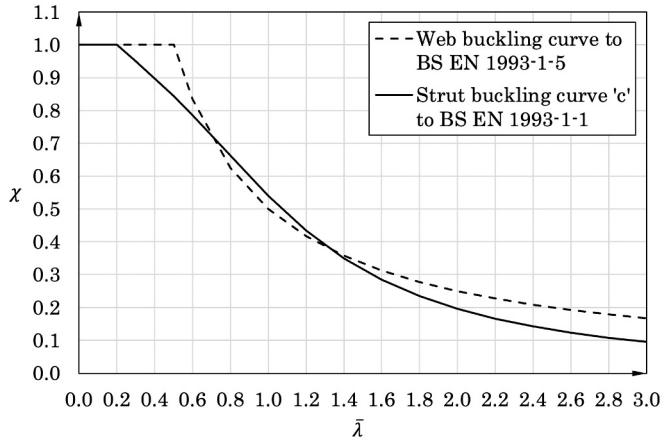

Fig. 1. Comparison between plate buckling and strut buckling curve "c" for various web slenderness ratios.

As the load from each jack is distributed equally to adjacent web-posts, the transverse compression force acting on the web-post is taken in the early part of the test as equal to the load from a single jack, P_{jack}. This leads to a compressive stress, σ_w, at the narrowest section of the web-post. However, when buckling of the web-post occurs and plasticity develops in the web-flange Tees, load is redistributed from the web-post by *Vierendeel* bending of the Tees. This leads to a significant post-buckling resistance in the test, which was investigated based on the FE analysis of the load case.

The measured dimensions and material properties of the tested beam are summarised in Table 1. The cellular beam proportions are within the limits of application of BS EN 1993-1-13 [2].

This cellular beam had previously been used in an earlier study by the authors [7], where it was tested under a different loading arrangement that focused on the behaviour of the end-posts next to the beam-to-column connections. However, for the present investigation, the zone of interest was located near mid-span – well away from regions affected by the previous loading – allowing the specimen to be reused without compromising the validity of the results.

The instrumentation layout is shown in Fig. 2 (d). Vertical deflections of the top and bottom flanges at the web-post centreline were recorded by potentiometers M1 and M2, respectively. The difference between M1 and M2 was used to measure the vertical shortening of the web-post resulting from local buckling.

Additional vertical deflections were captured at the locations of the two applied loads using potentiometer pairs V1–V2 and V3–V4. The difference between V1 and V2 (and likewise between V3 and V4) was used to capture in-plane rotation of the top Tees.

Out-of-plane horizontal displacement due to web-post buckling was measured at mid-height of the web using dial gauge H1. Although the intended measurement location was on the centreline of the web-post, the gauge was placed slightly closer to the adjacent opening due to spatial constraints caused by the mid-span restraint.

4. Finite element analysis of web-post buckling

The web-post buckling resistance of the cellular beam to transverse loads was investigated using Abaqus [8]. The starting point was to analyse the behaviour of the test beam and its loading, and then to use the calibrated model to extend to a parametric study of transverse load applied directly above the web-post. The modelling approach began with a linear buckling analysis (LBA), also referred to as eigenvalue analysis, using the "Buckle" step in Abaqus. This step identifies the critical buckling load and the corresponding buckling mode.

Following this, a geometrically and materially non-linear analysis with imperfections (GMNIA) was conducted using the "Static, Riks" step in Abaqus. The eigenvalues obtained from the LBA were used as reference loads in this subsequent step. The modified Riks method is a well-established approach for solving geometrically nonlinear problems, particularly in cases where buckling leads to negative stiffness in the load-displacement response. It enables the identification of static equilibrium states even during unstable phases, making it suitable for analysing structural behaviour beyond initial buckling [9].

4.1. Details of the FE models

The geometry of all steel parts (web, flanges, stiffeners) was simulated using 4-node, linear, quadrilateral, doubly curved thin or thick shell elements with reduced integration, enhanced hourglass control, conventional stress/displacement, and finite membrane strains (S4R). The fillet weld between the flanges and web was not explicitly modelled, as its influence on web-post buckling was considered negligible in this context.

The constitutive material models used for the steel beam included both linear elastic and bi-linear models. In the LBA, the steel was

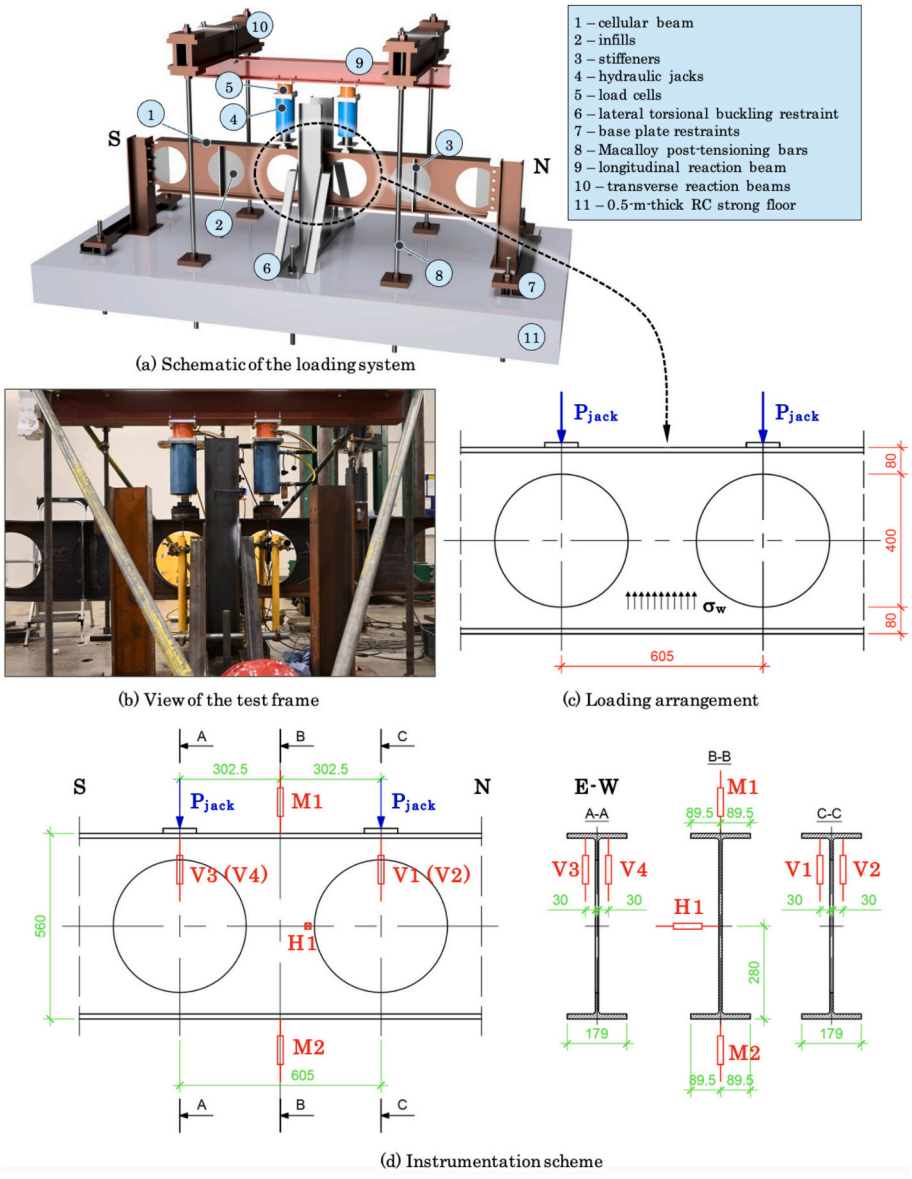

Fig. 2. Details of the test setup (units: millimetres).

Table 1
Measured details of the cellular beam test.

Dimension	Symbol	Value (units)
Beam depth	h	560 mm
Flange width	b_f	179 mm
Opening diameter	h_o	400 mm
Centre-to-centre spacing	s	605 mm
Web-post width	s_o	205 mm
Web thickness	t_w	9.0 mm
Flange thickness	t_f	14.2 mm
Root radius	r	10.2 mm
Steel yield strength	f_y	393 N/mm^2

assumed to exhibit linear elastic stress-strain behaviour, with Young's modulus $E = 210\ GPa$ and Poisson's ratio $\nu = 0.3$. For the GMNIA, plasticity was introduced using a bi-linear model with kinematic hardening.

In the validation study, the material properties were based on certification data, with a yield strength $f_y = 393$ N/mm^2 and an ultimate tensile strength $f_u = 511$ N/mm^2. For the later parametric FEA study, nominal material properties were assumed for steel grades S355 and S450, as specified in BS EN 1993-1-1 [3]. The yield strain was determined as $\varepsilon_y = f_y/E$ and the ultimate strain was estimated as $\varepsilon_u = 0.6\left(1 - f_y/f_u\right)$, as proposed by Yun and Gardner [10]. Nominal (engineering) stresses and strains were then converted to true (Cauchy) stress and logarithmic strain for use with the finite strain formulation in Abaqus [9].

Details of the boundary conditions and applied loads are shown in Fig. 3. The end supports were simulated using reference points positioned notionally at the centreline of the columns, which were coupled to the beam ends through kinematic coupling constraints. Pin supports were then assigned to these reference points to replicate the boundary conditions. Loads were applied to reference points located 25 mm above the flange, which were coupled to the flange using kinematic coupling over a 100 mm × 100 mm area of the plate placed on the top flange.

In the LBA step, unit loads were applied (CF2 = −1 in Abaqus) as only a reference load is required to determine the eigenvalues and corresponding buckling modes. In the GMNIA step, these unit loads were replaced with the eigenvalue obtained for the fundamental eigenmode. In the validation study, two loads were applied over the openings (Fig. 3

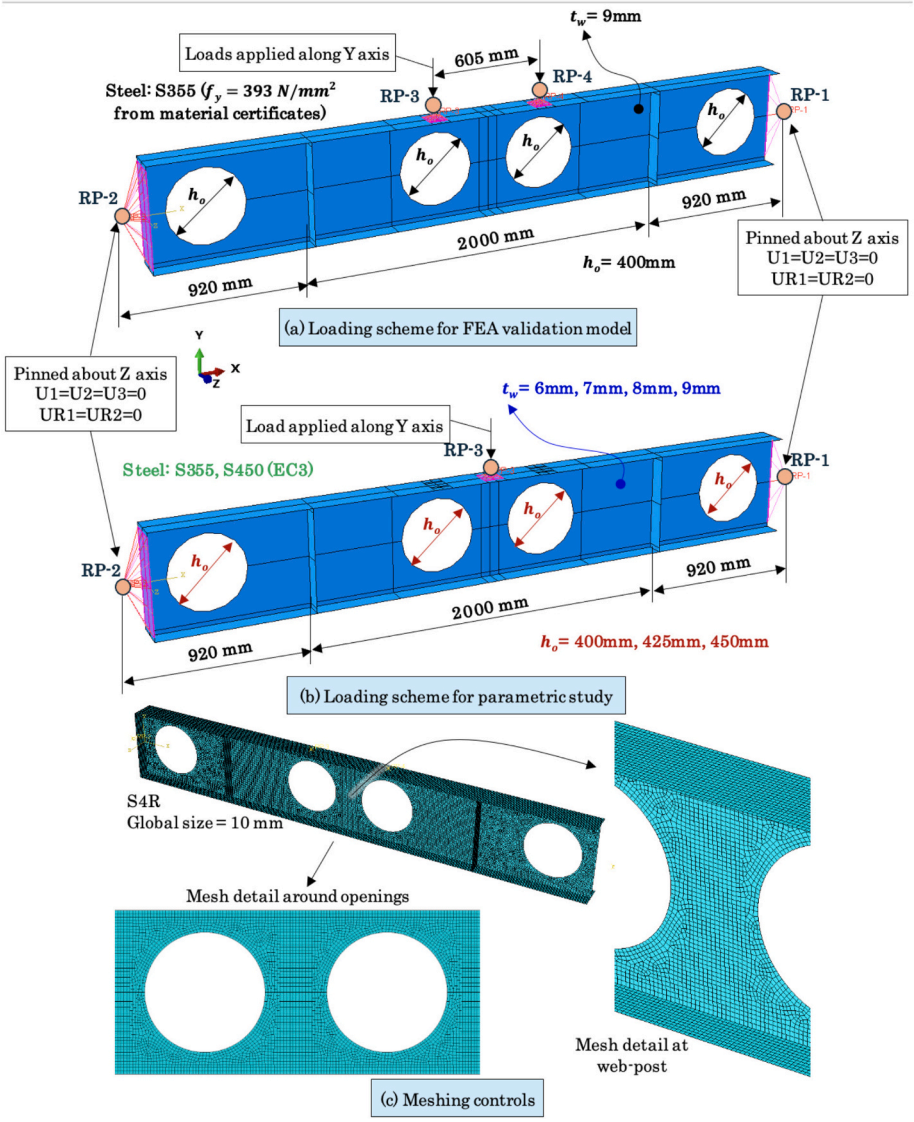

Fig. 3. Details of the FE models of the cellular beams.

(a)), whereas in the parametric FEA, a more representative case was modelled with a single transverse load applied directly over the web-post (Fig. 3 (b)).

No restraints were applied to the top flange or to the reference points used for the loads. While this differed from the experimental setup, where a lateral restraint was present to prevent lateral-torsional buckling, additional restraints in the model resulted in a response that was excessively stiff compared to the test. It was concluded that the global buckling modes did not govern. This was further confirmed by the FEA validation study, which consistently showed that the fundamental buckling mode remained web-post buckling, even without restraining the top flange against lateral-torsional buckling (Fig. 4).

Following a mesh refinement study, the final mesh, as shown in Fig. 3 (c), was generated using a global element size of 10 mm, with its distribution influenced by the specific partitioning of the model. This configuration was deemed to provide the best balance between accuracy and computational efficiency, ensuring good convergence for the GMNIA while maintaining a reasonable execution time.

4.2. Results of the linear buckling analysis

The GMNIA was performed on a perturbed geometry of the beam by introducing an initial imperfection coupled to the relevant eigenmode. The results of the linear buckling analyses used to define the perturbed geometry are shown in Fig. 4 and Fig. 5. These include the buckling modes and corresponding buckling loads for both the FEA validation model, based on the test arrangement, and a representative case from the parametric study with a single point load applied above the web-post. The selected parametric model is for a cellular beam with h_o = 400 mm, t_w = 9 mm, and using S355 steel.

Fig. 4 shows that, for the model representing the test arrangement, the eigenvalue of the second mode is approximately 36 % higher than that of the first (fundamental) mode. This confirms that mode 1 is dominant and would be reached well before the load level required to activate mode 2 for lateral torsional buckling.

When comparing the model representing the test arrangement to the parametric model in Fig. 5, it is evident that transitioning from two loads over the openings to a single load directly above the web-post does not result in a simple doubling of the buckling load. This indicates the development of a different structural mechanism, which develops more of the web's bending resistance, particularly in the web-flange Tee sections above the adjacent openings. This behaviour is further illustrated by the cross-sections on the right-hand side of each figure, where the deformed shape associated with the first buckling mode mobilises a

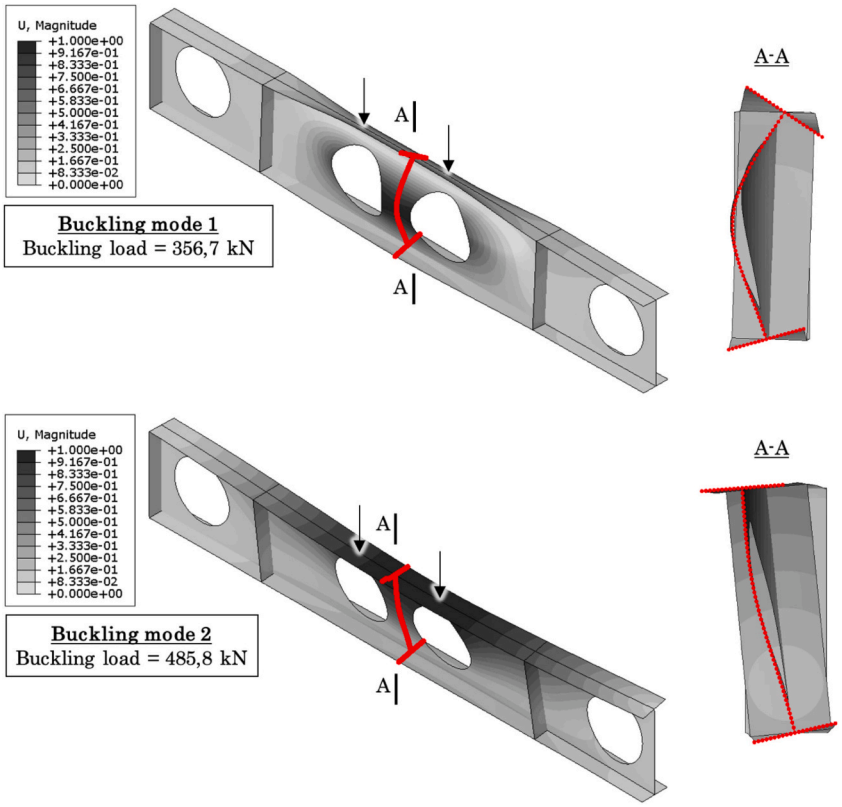

Fig. 4. Buckling modes for the test arrangement (in which the buckling load is the load corresponding to each load point and deformation scale factor = 100).

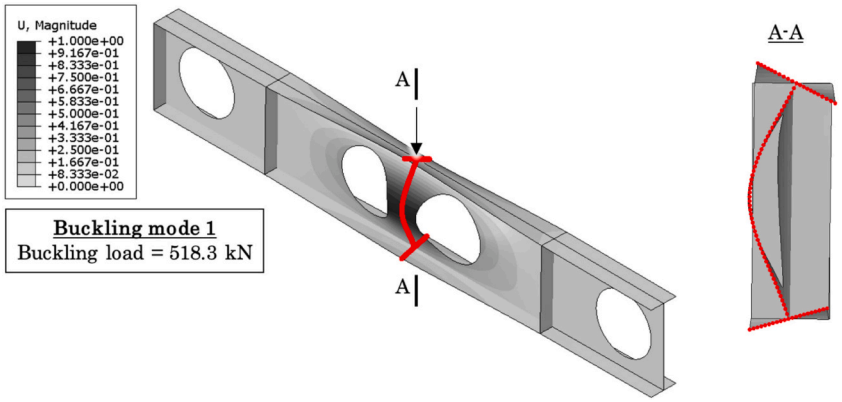

Fig. 5. Buckling modes for the case of a single point load (in which the buckling load is the load corresponding to the load point and deformation scale factor = 100).

larger portion of the web surrounding the openings in the test arrangement than in the single-point load case.

Also, when load is applied directly above the web-post, local bending of the Tees occurs on both sides of the web-post, whereas in the test load case, local bending of the Tees mainly occurs on one side of the opening. In the later model of web-post buckling, the additional resistance due to local bending of the Tees is separated from the buckling resistance of the web-post as bending of the Tees is essentially a post-buckling resistance caused by shortening of the web-post as it buckles.

4.3. Initial geometric imperfection and residual stress

Since in all cases examined in this study the first eigenmode corresponded to web-post buckling, only this mode was considered when defining the perturbed geometry for the imperfection analysis. From the FEA validation study, the appropriate imperfection magnitude was determined as $\delta_w = h/100$ (5.6 mm), where h is the beam depth of 560 mm. This relatively large imperfection was necessary to achieve close agreement with the test results, potentially due to residual deformations from the previous test or unintended effects from the test setup.

However, for the parametric FEA study, a more conventional imperfection magnitude was adopted, with an initial out-of-plane deformation of the web-post equal to $\delta_w = h/200$ (2.8 mm). This choice aligns with the imperfection values proposed by Teixeira et al. [11] for web bending, providing a basis for a generalised assessment of web-post stability.

Residual stresses were considered in a control FE model to assess their influence on web-post buckling resistance. The residual stress distribution adopted in this paper followed the profile proposed by Sonck et al. [12–14] for cellular beams, applicable for sections with a depth-to-width ratio of the original parent section h'/b > 1.2 and assuming a standard fabrication process. For the cellular beam used in

this study which is rewelded from a 406 × 178 × 67 kg/m UB, h'/b = 2.3. In this profile, the residual stress pattern shown in Fig. 6 (a) was determined using Eq. 6.5.1 from Sonck [12]. The stresses were introduced in Abaqus via the keyword editor as initial conditions, together with the geometric imperfection, before the GMNIA step. A predefined stress state (*INITIAL CONDITIONS, TYPE = STRESS) was applied using sets of mesh elements running along the length of the beam, with varying stresses assigned across the width of the flange and the web according to the above profile.

The comparison between FE results with and without residual stresses presented in Fig. 6 (b) is based on the horizontal out-of-plane deflection at mid-width and mid-height of the web-post, which confirmed that their inclusion has a negligible effect on the overall web-post buckling resistance. Based on this finding, residual stresses were omitted from the parametric study models.

4.4. Test results and validation of the numerical model

From the FEA validation study, Fig. 7 shows the rotation of the top Tee at the centreline of the opening, and Fig. 8 illustrates the corresponding vertical shortening (M1–M2) and horizontal deflection (H1) at the centreline of the web-post. The values plotted on the total applied load axis (sum of the jack loads) were computed as the product of the load proportionality factor (LPF) from the GMNIA and the eigenvalue of the fundamental mode from the LBA, which served as the reference elastic buckling load in the GMNIA step (e.g., for eigenmode 1, elastic buckle load = 518 kN, while $F_w = LPF \times 518$ kN). The close agreement between the FEA predictions and the test measurements confirms the validity of the modelling approach and supports its application in the subsequent parametric study. As noted earlier, the compression force transferred to the web-post is in theory half of the sum of the jack forces up to the point of buckling of the web-post.

Having validated the FE model, Fig. 9 shows the web-post buckling resistance relative to the load per jack for the test case with loads applied above adjacent openings. It can be seen that the ratio of the web-post buckling resistance to the load per jack at the buckling load is 0.44. However, the FE analysis continued to a failure load of 254 kN at larger displacements, which indicated an 18 % post-buckling reserve due to plasticity in the Tees remote from the buckled web-post.

To interpret the buckling behaviour of the web-post, it is necessary to separate the buckling resistance of the web-post from the post-buckling bending of the Tees, which cannot necessarily be relied on to resist transverse loads when combined with the effects of vertical shear in the general design of a cellular beam.

The method for determining the web-post buckling resistance at the onset of buckling $N_{wp.b.FEA}$ and the total transverse load corresponding to web-post buckling $F_{w.FEA}$ from FEA is detailed in the next section for the parametric study.

5. Parametric study of web-post buckling resistance for transverse load applied above the web-post between circular openings

5.1. Parametric study and design assumptions

To support the development of improved design expressions for web-post buckling, a parametric finite element analysis (FEA) study was carried out for the design case of transverse load applied to the centreline of the web-post. This study builds on the validated FE model and explores a range of opening diameters, h_o, web thicknesses, t_w, and steel grades, as summarised in Table 2. All cases except

$t_w = 6mm$ in S450 steel satisfy the web slenderness limit

$h_w = 121 t_w \epsilon$ in BS EN 1993-1-13 [2] and cover a practical range of application of cellular beams.

The aim is to provide a consistent and practical dataset for cellular beams with which to assess the accuracy of two possible design approaches: (i) the plate buckling model in BS EN 1993-1-5 [1], and (ii) the equivalent strut buckling method using buckling curve 'c' in BS EN 1993-1-1.

Each case is assessed by computing the compressive force in the web-post at the onset of buckling, $N_{wp.b.FEA}$, and comparing this with design predictions.

The buckling resistance of the web-post, denoted as $N_{wp.b.FEA}$, was determined by first identifying the analysis increment at which the compressive stress in the web-post reached its maximum. The increment at which $\sigma_{c.wp.b.FEA}$ reached its maximum value was taken to indicate the onset of buckling, beyond which the web-post no longer sustained additional load. This stress, $\sigma_{c.wp.b.FEA}$, was calculated using the difference between the peak compressive and tensile vertical stresses across the thickness of the web-post, as given by Eq. (14):

$$\sigma_{c.wp.b.FEA} = \frac{|\sigma_c| - \sigma_t}{2} \tag{14}$$

Where σ_c is the compressive stress and σ_t is the tensile stress

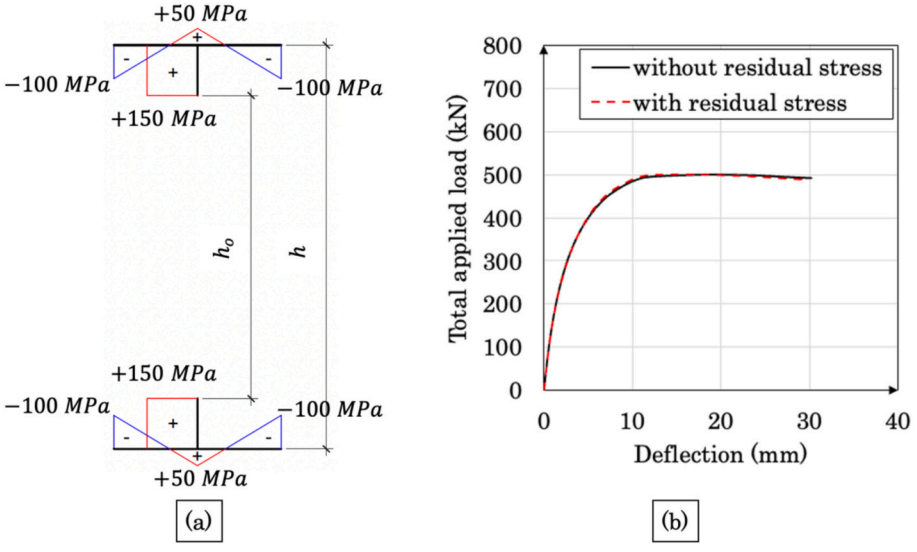

Fig. 6. Residual stresses: (a) pattern for cellular beams based on Sonck [12], (b) comparison of load-displacement curves for the case of h_o = **425** mm, s_o = **180** mm, t_w = **7** mm, and S355 steel, with and without residual stresses.

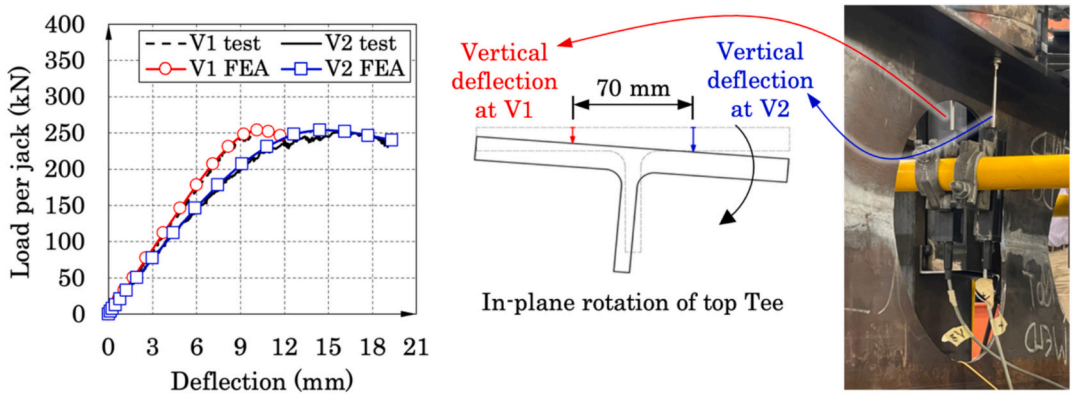

Fig. 7. Test results and FEA validation showing rotation of the top Tee at centreline of the opening.

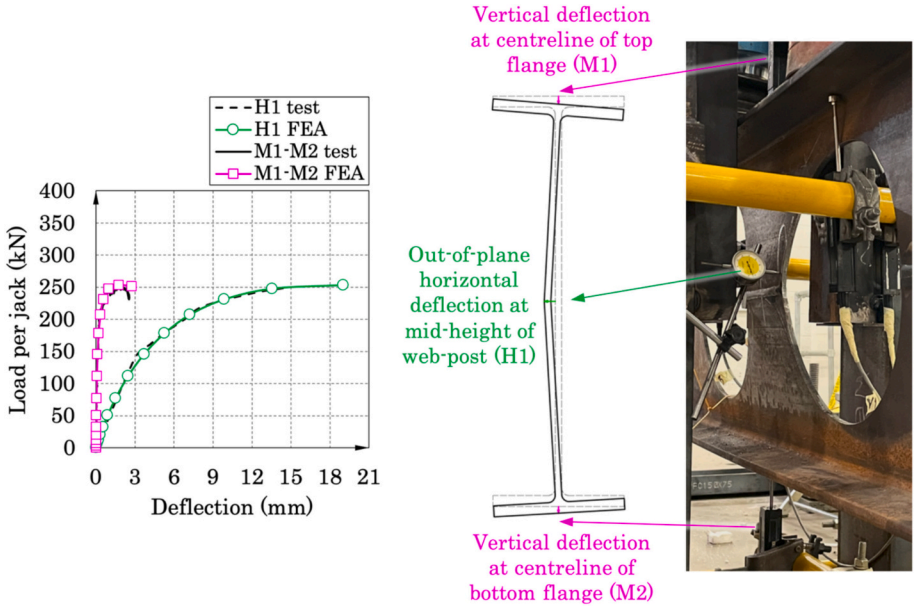

Fig. 8. Test results and FEA validation showing vertical shortening (M1-M2) and horizontal deflection (H1) at centreline of the web-post.

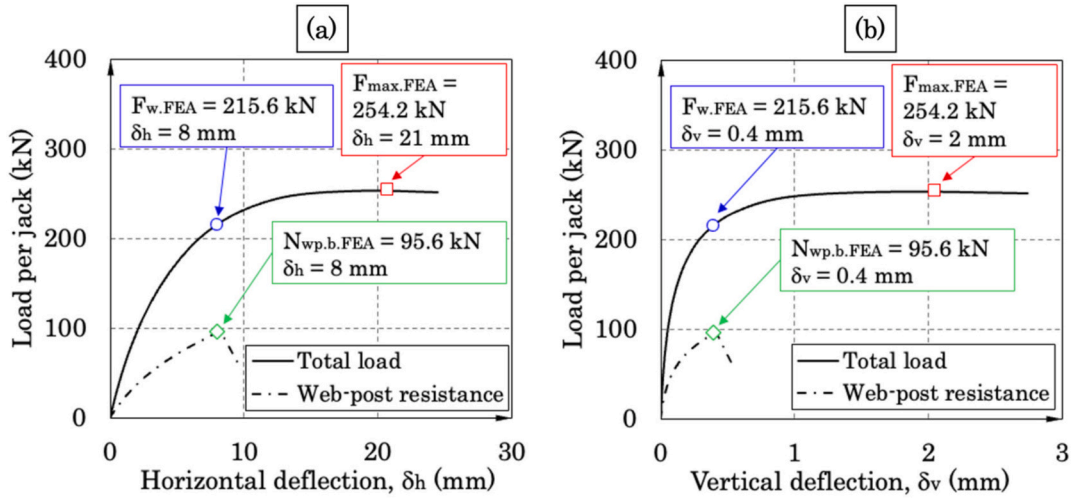

Fig. 9. Analysis of loading versus displacement curves from FEA model of the test.

Table 2
Overview of variables considered in the parametric study.

Parameter matrix	$h_o = 400mm$, $s_o = 205mm$		$h_o = 425mm$, $s_o = 180mm$		$h_o = 450mm$, $s_o = 155mm$	
	S355	S450	S355	S450	S355	S450
$t_w = 9mm$	•	•	•	•	•	•
$t_w = 8mm$	•	•	•	•	•	•
$t_w = 7mm$	•	•	•	•	•	•
$t_w = 6mm$	•	•	•	•	•	•

Note: $h_w = 532\ mm$ is constant in the parametric study.

measured on opposite sides of the web-post (as shown for the node at the middle of the web-post width in Fig. 10).

However the distribution of the compressive stresses across the web-post is non-uniform and Fig. 11 presents the stress profile across a 205 mm wide web-post width for all thicknesses and steel grades. This was repeated for all cases, and it was found that the difference between the maximum and minimum stresses increased as the steel thickness reduced, which implies an effect of the local flexibility at the edge of the opening for slender webs. The ratio of the average compressive stress, $\sigma_{c.wp.av}$, to the maximum stress also defines the effective width of the web-post relative to the actual width. For design purposes, this is given in Eq. (15) with reasonable accuracy over the range of web thicknesses and strengths as:

$$s_{o,eff} = 0.4s_o + 16t_w\varepsilon \leq s_o \tag{15}$$

This means that the effective web-post width is less than the actual width when $s_o > 27t_w\varepsilon$, which although approximate, leads to reasonably accurate results when used in the web-post buckling method derived later.

At the load corresponding to the onset of buckling, the compressive force resisted by the web-post was computed from the FEA using the average compressive stress, $\sigma_{c.wp.av}$, as per Eq. (16):

$$N_{wp.b.FEA} = \sigma_{c.wp.av}t_w s_o = \sigma_{c.wp.max}t_w s_{o,eff} \tag{16}$$

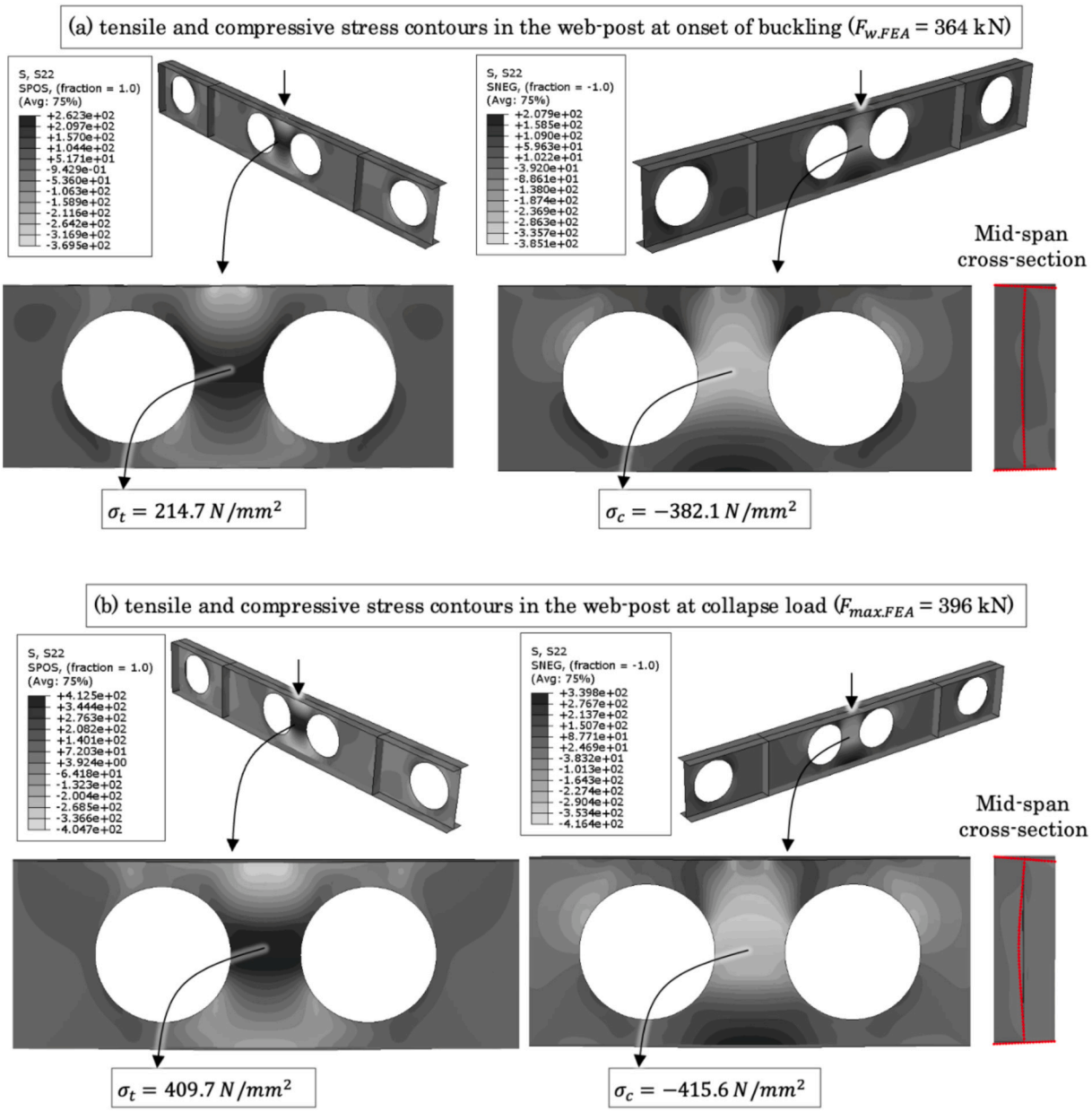

Fig. 10. Vertical stress contours in the web-post (the case of $h_o = 400mm$, $s_o = 205mm$, $t_w = 9mm$, and S355 steel).

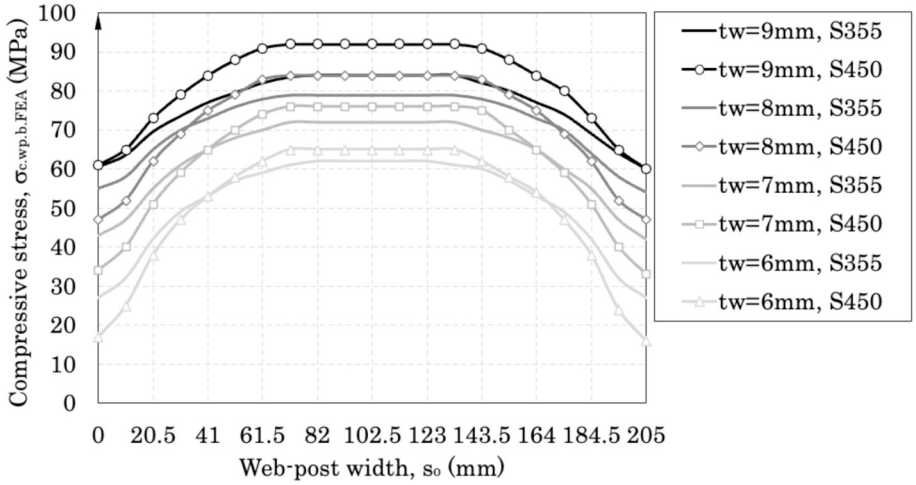

Fig. 11. Compressive stress profiles across the web-post width obtained from the FEA (for $h_o = 400mm$ and $s_o = 205mm$).

As noted, the web-post buckling resistance, $N_{wp.b.FEA}$, is less than the total transverse load, $F_{w.FEA}$. Buckling of the relatively slender web-post leads to shortening along its vertical axis which leads to local bending of the adjacent Tees in their elastic range. The pure buckling resistance of the web-post is separated from the resistance due to local bending of the Tees in the design model presented later.

This distinction between $N_{wp.b.FEA}$ and the total transverse load $F_{w.FEA}$ at the onset of buckling is illustrated in Fig. 12, where the loading versus displacement curves are presented as:

- Fig. 12 (a) plots the total applied transverse load against the out-of-plane horizontal displacement δ_h at the mid-height of the centreline of the web-post.
- Fig. 12 (b) shows the total applied transverse load versus the vertical shortening δ_v, derived from the relative vertical displacements at mid-span, attributed to web-post buckling.

In this case, the web-post buckling resistance is determined as 38 % of the applied load at the point of buckling of the web-post. Both curves also show the maximum transverse load, $F_{max.FEA}$, reached during the nonlinear analysis, which is 9 % higher than the transverse load at the onset of buckling $F_{w.FEA}$. As noted, the difference between these two values arises from plasticity in the adjacent Tees as shown by the softer yet rising segment of the load–displacement curve beyond the buckling point.

While $F_{max.FEA}$ is marked in the figures for completeness, the development of the design expressions in this study is based on the more conservative buckling threshold, represented by $F_{w.FEA}$, rather than the ultimate load in the FE study.

The results of the parametric study are summarised in Tables 3 to 5. The average compressive stresses in the web-posts at the onset of buckling, $\sigma_{c.wp.av}$, are presented in Table 3, showing a slight increase with increasing opening diameter and reduced web-post width. These buckling stresses typically ranged between 49 and 97 N/mm^2.

The corresponding web-post buckling resistances, $N_{wp.b.FEA}$, calculated using Eqs. (14) and (16), are given in Table 4. These values typically represent between 26 % to 44 % of the total applied load at failure.

Table 3
Average compressive stress in the web-post at the onset of buckling.

Average compressive stress, $\sigma_{c.wp.av}$(N/mm^2)	$h_o = 400mm$ $s_o = 205mm$		$h_o = 425mm$ $s_o = 180mm$		$h_o = 450mm$ $s_o = 155mm$	
	S355	S450	S355	S450	S355	S450
$t_w = 9mm$	76	81	82	88	92	97
$t_w = 8mm$	71	71	76	81	82	88
$t_w = 7mm$	62	62	66	69	74	76
$t_w = 6mm$	50	49	55	56	61	64

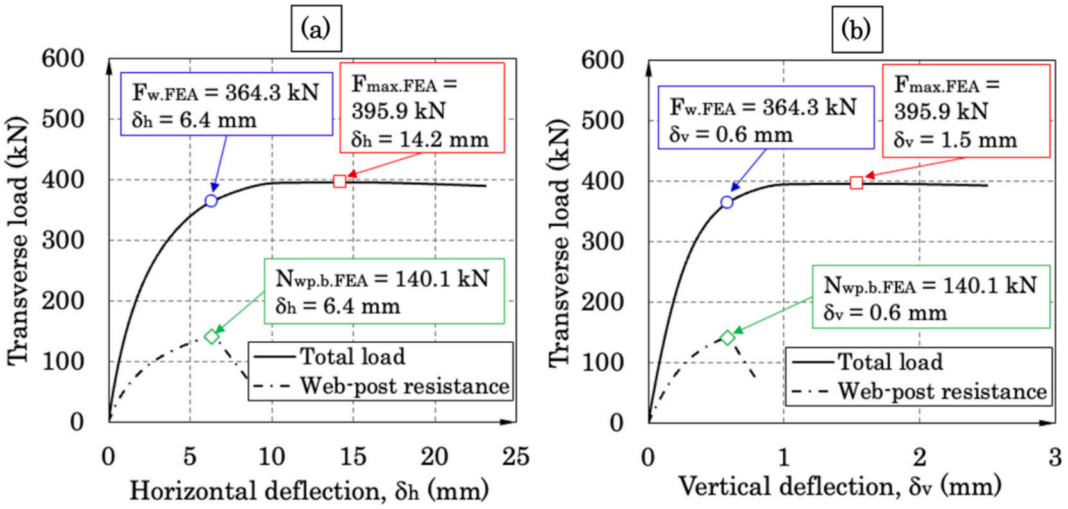

Fig. 12. Loading vs. displacement curves from FEA (the case of $h_o = 400mm$, $s_o = 205mm$, $t_w = 9mm$, and S355 steel).

Table 4
Web-post buckling resistance calculated from the web-post stresses in Table 3.

Web-post buckling resistance, $N_{wp.b.FEA}$ (kN)	$h_o = 400mm$ $s_o = 205mm$		$h_o = 425mm$ $s_o = 180mm$		$h_o = 450mm$ $s_o = 155mm$	
	S355	S450	S355	S450	S355	S450
$t_w = 9mm$	140	149	133	143	128	136
$t_w = 8mm$	117	117	110	117	102	109
$t_w = 7mm$	89	89	83	86	80	83
$t_w = 6mm$	61	60	59	60	57	59

Table 5
Total transverse load at the point of web-post buckling obtained from FEA.

Total transverse load, $F_{w.FEA}$ (kN)	$h_o = 400mm$ $s_o = 205mm$		$h_o = 425mm$ $s_o = 180mm$		$h_o = 450mm$ $s_o = 155mm$	
	S355	S450	S355	S450	S355	S450
$t_w = 9mm$	364	402	324	360	280	312
$t_w = 8mm$	307	341	273	302	236	262
$t_w = 7mm$	253	283	224	250	192	214
$t_w = 6mm$	203	228	177	198	150	167

For comparison, the total transverse loads at the onset of buckling, $F_{w.FEA}$, obtained from the full nonlinear FEA simulations, are presented in Table 5. The difference between $N_{wp.b.FEA}$ and $F_{w.FEA}$ is attributed to local bending of the adjacent top Tees, as previously discussed.

5.2. Web-post buckling resistance using plate buckling curve to BS EN 1993-1-5

As noted in Section 5.1, the combined failure load of the two jacks in the test and FEA includes contributions from both web-post buckling and bending of the Tees on the high shear side. However, to establish a rational and conservative design method, it is essential to first isolate the contribution of the web-post alone. This provides a consistent basis for treating the web-post as a slender plate in compression, in line with BS EN 1993-1-5 [1].

The plate buckling curve defined in BS EN 1993-1-5 [1] for transverse loading is given by Eq. (17):

$$\chi_{wp} = \frac{0.5}{\bar{\lambda}_{wp}} \tag{17}$$

The parameter that determines the buckling resistance is the plate buckling coefficient, k_f. The relationship between the effective length of a notional strut and k_f for plate buckling is given from Eqs.(2) and (3) by Eq. (18):

$$l_{eff} = 0.95 h_w \, k_f^{-0.5} \tag{18}$$

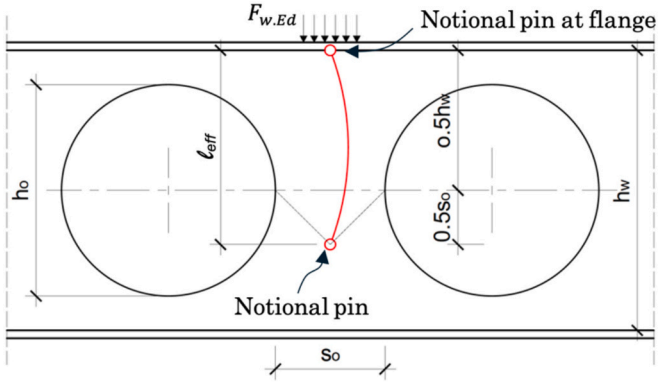

Fig. 13. Mechanical model showing proposed effective length for web-post buckling using equivalent strut buckling method to BS EN 1993-1-1.

The proposed effective buckling length of the web-post ignoring the torsional restraint of the beam flange is illustrated in Fig. 13. This has notional pin connections at the top flange and at a distance $0.5s_o$ below the centreline of the openings. Therefore, the effective length of the notional strut is taken as Eq. (19):

$$l_{eff} = 0.5(h_w + s_o) \tag{19}$$

When expressed in terms of the plate buckling coefficient, an alternative expression that provides equivalent results to the effective length formula given in Eq. (19) is shown in Eq. (20):

$$k_f = 2(1 - s_o/h_w) \text{ but } k_f \geq 1 \tag{20}$$

For wider web-posts with $s_o > 0.5h_w$, the plate buckling coefficient is taken as 1.0, when using this method.

In addition, the FEA showed that the stress distribution across the web-post is non-uniform. For simple design of cellular beams, the effective width of the web-post in compression may be taken as $s_{o,eff} = 0.85s_o$. This applies for web-post widths, $s_o \leq 0.51h_o$ and web slenderness, $h_w \leq 121t_w\varepsilon$, corresponding to the practical range of this study.

A more accurate formula for the effective web-post width over the range of web-post widths and slenderness is given by Eq. (15).

For detailed calculations of the web-post buckling resistance using plate buckling curve to BS EN 1993-1-5 [1], refer to the Annex.

Inserting k_f from Eq. (20) into the expression for the relative slenderness of the web in Eq. (3) and using the plate buckling curve in Eq. (17) gives a relatively simple formula for the design buckling resistance of the web-post subject to transverse load in Eq. (21):

$$N_{wp.b.Rd} = 20t_w^2\varepsilon(s_{o,eff}/h_w)(1 - s_o/h_w)^{0.5} f_y \tag{21}$$

Where $s_{o,eff}$ is given by Eq. (15) and $s_{o,eff} \leq s_o$.

The web-post buckling resistances obtained from Eq. (22) with $s_{o,eff}$ given by Eq. (15) are presented in Table 6, which shows good accuracy over the range of web-post widths and slenderness in this study.

For these cases, Table 7 gives the ratios of the global moment acting at the centreline of the adjacent opening from the transverse load corresponding to web buckling to the theoretical bending resistance of the cellular beam cross-section. The moment ratio is in the range of 0.23 to 0.46 and based on the interaction in Eq. (5), the moment effect can be ignored when interpreting these FEA results. Table 7 also gives the effect of the shear force to the shear resistance of the cellular beam which is in the range of 0.41 to 0.59. A shear ratio less than 0.5 does not affect the local bending resistance of the Tee. However, if a higher proportion of the applied shear is resisted by the top Tees, then the shear ratio for the top Tees will increase and will have an effect on their local bending resistance. In the proposed model, the bending resistance of the Tees is limited to its elastic resistance and is only included as a post-buckling effect.

5.3. Web-post buckling resistance using the alternative equivalent strut method to BS EN 1993-1-1

While the plate buckling method aligns more directly with the

Table 6
Ratio of predicted buckling resistance to BS EN 1993-1-5 to FEA-derived buckling resistance.

$\frac{N_{wp.b.Rd}}{N_{wp.b.FEA}}$	$h_o = 400mm$ $s_o = 205mm$		$h_o = 425mm$ $s_o = 180mm$		$h_o = 450mm$ $s_o = 155mm$	
	$k_f = 2(1 - s_o/h_w)$ and $s_{o,eff} = 0.4s_o + 16t_w\varepsilon \leq s_o$					
	S355	S450	S355	S450	S355	S450
$t_w = 9mm$	0.98	0.97	0.97	0.99	0.90	0.95
$t_w = 8mm$	0.87	0.91	0.91	0.89	0.89	0.93
$t_w = 7mm$	0.81	0.86	0.85	0.87	0.86	0.87
$t_w = 6mm$	0.80	0.87	0.81	0.84	0.81	0.82

Table 7
Global bending moment and shear force ratios at the centreline of the adjacent openings from the results of the parametric study.

Web thickness	Utilisation in FEA model	$h_o = 400mm$		$h_o = 425mm$		$h_o = 450mm$	
		S355	S450	S355	S450	S355	S450
$t_w = 9mm$	Moment ratio	0.46	0.40	0.42	0.37	0.38	0.33
	Shear ratio	0.55	0.48	0.58	0.51	0.59	0.52
$t_w = 8mm$	Moment ratio	0.40	0.35	0.36	0.32	0.32	0.28
	Shear ratio	0.51	0.45	0.53	0.46	0.55	0.48
$t_w = 7mm$	Moment ratio	0.33	0.29	0.30	0.26	0.27	0.23
	Shear ratio	0.47	0.41	0.47	0.41	0.49	0.43

Eurocode provisions for transverse loading, this study also explored the suitability of an equivalent strut buckling model based on BS EN 1993-1-1 [3]. This comparison is particularly relevant for narrow web-posts, which may exhibit strut-like behaviour.

For this purpose, the effective length proposed in combination with buckling curve 'c' from BS EN 1993-1-1 [3] is given by Eq. (19). The predicted web-post resistances were compared against FEA results, as summarised in Table 8.

The results show that the equivalent strut method is slightly unconservative for $t_w = 9mm$ and becomes more conservative for more slender webs compared to the plate buckling method due to the difference in the shape of the buckling curves in Fig. 1. It is concluded that the plate buckling model in BS EN 1993-1-5 [1] gives more consistent agreement across the parametric study.

5.4. Observed contributions from Tee bending

To investigate the transverse load resistance due to local bending of the Tees adjacent to the loaded web-post, Fig. 14 presents the von Mises stress distributions in the Tees for the stated case and at the failure load in the FEA , $F_{w.FEA}$.

The stress profiles are extracted at a representative cross-section located at a horizontal position of 0.35 h_o from the centreline of the opening. This position corresponds to the mid-length of an equivalent hexagonal opening with notional width, 0.7 h_o, as introduced in the mechanical model developed in Section 6.1, where circular openings are approximated as regular hexagons to facilitate analysis of local bending effects in the elastic range at the onset of web-post buckling. This equivalent opening width differs from that used for Vierendeel bending effects due to transfer of shear in BS EN 1993-1-13 [2], which would lead to a higher shear force acting in the top Tees.

The FEA stresses include the axial stresses due to the global bending moment and the local bending stresses due to the component of the transverse force acting in the top and bottom Tees across the openings. The von Mises stress values are averaged across both sides of the web and are used to calculate the stress development in the top and bottom Tees. At $F_{w.FEA}$, the stresses at this position are in the elastic range and the stress at the edge of the top Tee exceeds that in the bottom Tee, which means that more of the shear force is transferred by the top Tee.

These observations form the basis for the extended design model proposed in Section 6.

Table 8
Ratio of predicted strut buckling resistance to BS EN 1993-1-1 to FEA-derived buckling resistance.

$\frac{N_{wp.b.Rd}}{N_{wp.b.FEA}}$	$h_o = 400mm$ $s_o = 205mm$		$h_o = 425mm$ $s_o = 180mm$		$h_o = 450mm$ $s_o = 155mm$	
	$l_{eff} = 0.5(h_w + s_o)$					
	S355	S450	S355	S450	S355	S450
$t_w = 9mm$	1.01	0.93	1.01	0.96	0.97	0.95
$t_w = 8mm$	0.82	0.79	0.88	0.80	0.88	0.86
$t_w = 7mm$	0.69	0.67	0.74	0.69	0.77	0.71
$t_w = 6mm$	0.61	0.60	0.63	0.59	0.65	0.60

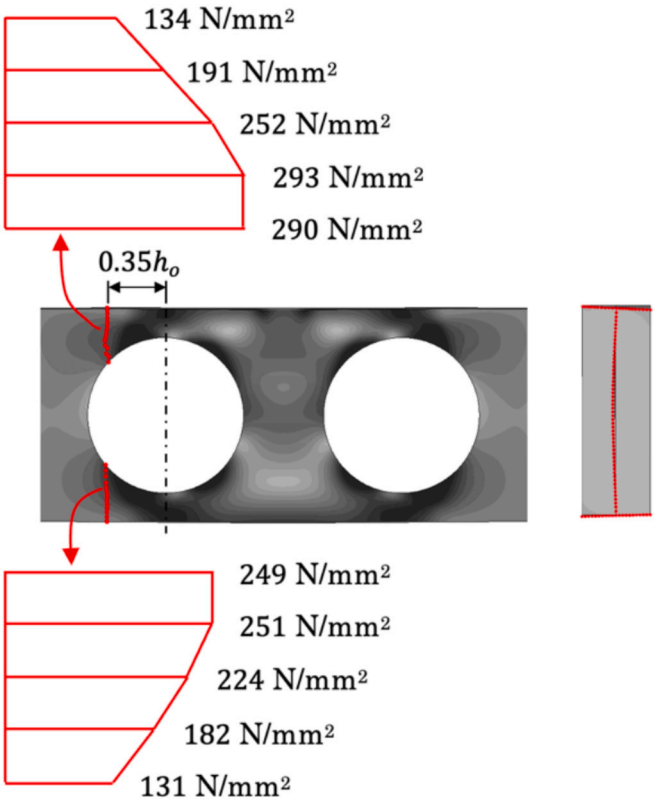

Fig. 14. Average Von Mises stress in Tees at onset of web-post buckling ($F_{w.FEA}$ = 364 kN, LPF = 0.74) (the case of $h_o = 400mm$, $s_o = 205mm$, $t_w = 9mm$, and S355 steel).

6. Extended design model for web-post buckling resistance to transverse loading applied to the centreline of the web-post

6.1. Proposed method based on force equilibrium

Buckling of the web-post due to a transverse load applied to the top flange at the centreline of the web-post leads to shortening of the web-post and to the development of bending moments in the top Tees in the adjacent openings. For double curvature bending of the top Tee over an equivalent opening length of a_{eq}, equilibrium of the shear forces is given by Eq. (22):

$$F_{w.Ed} = N_{wp.b} + 2V_T \tag{22}$$

Where $F_{w.Ed}$ is the transverse load applied to the web-post,

$N_{wp.b}$ is the buckling resistance of the web-post due to the transverse load,

And V_T is the shear force transferred by each of the adjacent top Tees.

The shortening of the web-post at the point of buckling is relatively small and so the simplified model is based conservatively on elastic bending of the Tees. Although the plastic bending resistance of the Tees increases with increasing deformation, the load resisted by the web-post in its post-buckled state will decrease, and so is outside the scope of the proposed method.

Therefore, the upper bound to the post-buckling resistance of the web-post in this simplified method takes the form shown in Eq. (23):

$$F_{w.Ed} \leq N_{wp.b} + \frac{4M_{el.Rd}}{a_{eq}} \tag{23}$$

Where a_{eq} is the equivalent opening length for deflection calculations across the opening,

And $M_{el.Rd}$ is the elastic bending resistance of the top Tee.

This equivalent opening width in this simplified model is derived from numerical integration of strains around the opening which is equated to the axial shortening of the web-post at the point of buckling of the web-post.

An equivalent hexagonal opening (Fig. 15) is defined in which the equivalent opening length for calculation of the deflection due to local bending of the top Tee across the adjacent openings is given by Eq. (24):

$$a_{eq} = 0.7h_o \tag{24}$$

The equivalent opening depth is taken as 0.9 h_o, so that the equivalent depth of Tee is given by Eq. (25):

$$h_{T.eq} = 0.5(h - 0.9h_o) \tag{25}$$

Where h is the beam depth.

In cellular beams, the web outstand area is generally less than 30 % of the flange area and parametric studies of typical T-sections show that the elastic bending resistance of a Tee in a rolled steel section, $M_{el.Rd}$, is given as a good approximation by Eq. (26):

$$M_{el.Rd} \approx \frac{t_w h_{T.eq}^{\ 2}}{3.5} f_y \tag{26}$$

Where $h_{T.eq}$ is the equivalent depth of the Tee.

Eqs. (23) to (26) reduce to an upper bound of the combination between the web-post buckling resistance and the bending of the Tees at the point of buckling given by Eq. (27):

$$F_{w.Rd} \le N_{wp.b.Rd} + 0.41 t_w \frac{(h - 0.9h_o)^2}{h_o} f_y \tag{27}$$

6.2. Comparison with FEA results

The proposed method is applied to all parametric cases previously modelled in FEA. The comparison includes predictions of the total transverse load using the extended model, evaluated using the same geometric and material parameters. The comparisons were made by combining the web-post buckling resistance with the additional transverse force resisted by the elastic bending of the Tees from Eq. (27). The resulting prediction-to-FEA ratios are presented in Table 9. A worked example is provided for the plate buckling case in the Annex.

The results in Table 9 show that the ratios of predicted resistance to transverse load, $F_{w.Ed}$, to the total transverse load from FEA, $F_{w.FEA}$, are in the range of 0.62 to 0.77. The method based in the elastic bending resistance of the Tees is reasonably consistent over the range of web-post widths and web thicknesses in the practical range of application This indicates that the simplified model of combined elastic bending in the Tees and buckling of the web-post is conservative.

However, as stated earlier, the inclusion of the local bending resistance of the Tees even in the elastic range, is not recommended for the design case with a more complex interaction of global shear and bending effects for a web-post also subject to a relatively high transverse load.

Table 9
Ratio of predicted total transverse load resistance to BS EN 1993-1-5 including elastic bending of the top Tees $F_{w.Rd}$ to FEA-derived total transverse loads $F_{w.FEA}$.

$\frac{F_{w.Rd}}{F_{w.FEA}}$	$h_o = 400mm$, $s_o = 205mm$		$h_o = 425mm$, $s_o = 180mm$		$h_o = 450mm$, $s_o = 155mm$	
	$k_f = 2(1 - s_o/h_w)$					
	S355	S450	S355	S450	S355	S450
$t_w = 9mm$	0.74	0.77	0.72	0.74	0.73	0.73
$t_w = 8mm$	0.71	0.75	0.68	0.71	0.68	0.69
$t_w = 7mm$	0.69	0.73	0.65	0.68	0.64	0.66
$t_w = 6mm$	0.67	0.72	0.64	0.67	0.62	0.65

Therefore, this first investigation of the resistance to transverse load in cellular beams should be continued, as indicated in Section 7.

7. Future research

The following topics for future research are identified as a result of this study on the resistance of cellular beams to transverse load:

7.1. Combined web-post shear, global moment and transverse forces

Transverse forces generally act in combination with global shear forces that lead to web-post buckling. This study did not investigate this effect, and it will be the subject of further research for cellular beams with closely spaced circular openings. A possible interaction formula is a linear combination between the buckling resistance of the web-post to a transverse force and web-post horizontal shear forces due to transfer of shear.

Transverse forces may also act in combination with high global moment for example in point loaded beams. Previous work [4] had led to an interaction formula for the effect of transverse loads and global moment which should be investigated for cellular beams.

7.2. Application to transverse load applied to the web below the top flange

In many design cases, secondary beams are connected to the primary cellular beam web. If the primary beam is much deeper than the incoming beam, the web is subject to transverse load that may cause web-post buckling determined by the stabilising effect of the connection and the position of the transverse load in the web depth.

This is clearly a more complex load case than load applied directly to the beam top flange, but it should be investigated.

7.3. Application to hexagonal and rectangular openings

Castellated beams have closely spaced hexagonal openings. The methodology for web-post buckling in cellular beams given in this paper can in principle be used for hexagonal openings, subject to further verification.

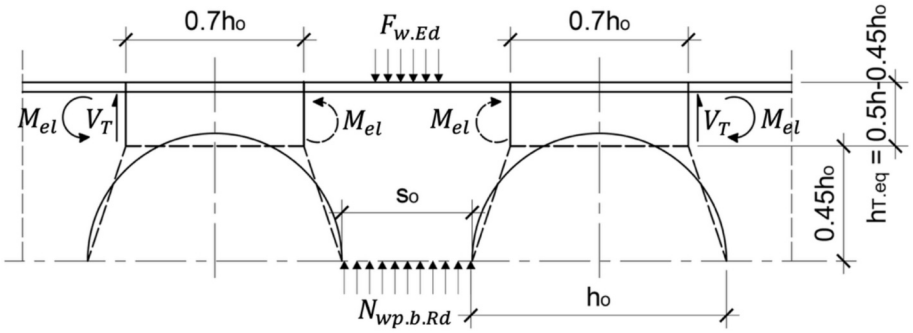

Fig. 15. Equilibrium of forces on web-post including *Vierendeel* bending of the top Tees.

Adjacent large rectangular openings require use of wider web-posts than cellular beams because of the transfer of horizontal shear forces. The methodology for resistance of web-posts between rectangular openings to transverse loads will differ in various respects:

- The dispersion of the transverse load to mid-height of the rectangular openings will lead to an effective width significantly less than the edge to edge spacing of the openings, as was identified for circular openings.
- The stabilising effect of the top Tees is reduced for rectangular openings and this should be investigated.
- For plate girders with rectangular openings, the potential range of web slenderness is greater than for cellular beams using rolled sections and the webs may be Class 4 to BS EN 1993-1-5.
- Rectangular openings may have horizontal stiffeners above and below the openings extending by an anchorage length outside the openings, which provide a partial stabilising effect to the web-post.

8. Concluding remarks

This study on the resistance of web-posts in cellular beams to the effect of transverse loads applied to the top flange showed that:

1. A load test on a 560 mm deep cellular beam with 400 mm diameter openings subject to jack loads applied above the centreline of adjacent openings failed at a load of 250 kN at each jack position, in which the compression in the web-post is theoretically equal to the jack load. Based on measured strains, it was determined that the web-post could resist an in-plane load of 96 kN at the point of buckling, and the post-buckling resistance was increased by local bending of the adjacent web-flange Tees, which is the more dominant effect.
2. The test arrangement was modelled using Abaqus with an initial imperfection of web height/100 which showed good agreement with the test.
3. Having validated the finite element model, a parametric study was made of the case of transverse load applied to the top flange at the centreline of the opening. The buckling resistance of the web-post was predicted with reasonable accuracy by a plate buckling coefficient $k_f = 2\,(1 - s_o/h_w)$, using the buckling curve to BS EN 1993-1-5. The model of an equivalent strut with an effective length $l_{eff} = 0.5(h_w + s_o)$ and using buckling curve 'c' to BS EN 1993-1-1 was less accurate over the range of web slenderness. In both cases, it is proposed that the effective width of the web-post may be taken as $s_{o.eff} = 0.4s_o + 16t_w\varepsilon$ (but $\leq s_o$) to take account of the non-uniform stresses across the web-post.
4. The force transfer by bending of the adjacent top Tees was predicted conservatively using a formula based on the elastic bending resistance of the Tees. Although this additional resistance occurs in FE models, it is ignored in determining the pure buckling resistance of the web-post.
5. The range of application of the study was for typical cellular beams using rolled sections with an opening diameter to depth ratio in the range of 0.7 to 0.8 and a web depth to thickness ratio in the range of 70ε to 120ε.
6. Further work is required to consider the effect of transverse loads on the web-posts between rectangular and hexagonal openings, and on the interaction between vertical shear and transverse loads.

CRediT authorship contribution statement

Konstantinos Daniel Tsavdaridis: Writing – review & editing, Validation, Supervision, Project administration, Methodology, Investigation, Funding acquisition, Data curation, Conceptualization. **Dan-Adrian Corfar:** Writing – original draft, Visualization, Validation, Software, Investigation, Formal analysis. **R. Mark Lawson:** Writing – review & editing, Validation, Supervision, Methodology, Investigation, Funding acquisition, Formal analysis, Data curation, Conceptualization.

Declaration of competing interest

None.

Appendix A. Annex: Web-post buckling resistance using plate buckling curve to BS EN 1993-1-5

A sample calculation is provided for the maximum transverse load applied to the web-post in a cellular beam using the buckling factor, $k_f = 2\,(1 - s_o/h_w)$ for $h_o = 400mm$, $s_o = 205mm$, $t_w = 9mm$, and S355 steel.

$$k_f = 2\left(1 - \frac{205}{532}\right) = 1.23$$

$$\bar{\lambda} = \frac{1}{28.4 \times 1.23^{0.5} \times 0.81}\left(\frac{532}{9.0}\right) = 2.31$$

$$\chi_{wp} = \frac{0.5}{\bar{\lambda}_{wp}} = \frac{0.5}{2.32} = 0.217$$

For the effective web-post width in Eq. (15):

$$s_{o,eff} = 0.4s_o + 16t_w\varepsilon = 0.4 \times 205 + 16 \times 9 \times 0.81 = 199mm = 0.97s_o$$

$$N_{wp.b.Rd} = \chi_{wp}s_{o,eff}t_w f_y = 0.215 \times 199 \times 9.0 \times 355 \times 10^{-3} = 138\ kN$$

Maximum web-post resistance obtained from FEA (Table 4): $N_{wp.b.FEA} = 140\ kN$

$$\frac{N_{wp.b.Rd}}{N_{wp.b.FEA}} = 0.98$$

Using the formula for the design buckling resistance in Eq. (21):

$$N_{wp.b.Rd} = 20 \times 9.0^2 \times 0.81 \times (199/532)(\,1 - 205/532)^{0.5} \times 355 \times 10^{-3} = 137\ kN$$

The FE analysis shows that the transverse resistance is increased by elastic bending of the top Tees, which is given by Eq. (27) as:

$$F_{w.Rd} \leq N_{wp.b.Rd} + 0.41 t_w \frac{(h - 0.9h_o)^2}{h_o} f_y = 137 + 0.41 \times 9 \times \frac{(560 - 0.9 \times 400)^2}{400} \times 355 \times 10^{-3} = 137 + 131 = 268\ kN$$

The transverse load from the FEA model is given as 364 kN in Table 5, showing that the simplified model is conservative but can predict the total transverse load with reasonable accuracy.

Data availability

No data was used for the research described in the article.

References

[1] BSI, Eurocode 3 - Design of Steel Structures. Part 1–5: Plated Structural Elements, BSI, London, 2024.
[2] BSI, Eurocode 3: Design of Steel Structures - Part 1–13: Beams with Large Web Openings, BSI, London, 2024.
[3] BSI, Eurocode 3: Design of Steel Structures - Part 1–1: General Rules and Rules for Buildings, BSI, London, 2023.
[4] O. Lagerqvist, B. Johansson, Resistance of I-girders to concentrated loads, J. Constr. Steel Res. 39 (1996) 87–119, https://doi.org/10.1016/S0143-974X(96)00023-5.
[5] T. Roberts, Slender plate girders subjected to edge loading, Proc. Inst. Civ. Eng. 71 (1981) 805–819, https://doi.org/10.1680/iicep.1981.1820.
[6] T.M. Roberts, F. Shahabian, Ultimate resistance of slender web panels to combined bending shear and patch loading, J. Constr. Steel Res. 57 (2001) 779–790, https://doi.org/10.1016/S0143-974X(01)00009-8.
[7] K.D. Tsavdaridis, B. McKinley, D.-A. Corfar, R.M. Lawson, Cellular beam end-posts with two connection types, end notches and infill plates, J. Constr. Steel Res. 215 (2024) 108547, https://doi.org/10.1016/j.jcsr.2024.108547.
[8] Dassault Systèmes SIMULIA Corp, Abaqus CAE, 2024, p. 2024.
[9] Dassault Systèmes SE, SIMULIA User Assistance 2024, Abaqus. Dassault Systèmes User Assistance, 2024. https://www.3ds.com/support/documentation/user-guides (accessed February 20, 2025).
[10] X. Yun, L. Gardner, Stress-strain curves for hot-rolled steels, J. Constr. Steel Res. 133 (2017) 36–46, https://doi.org/10.1016/j.jcsr.2017.01.024.
[11] F.B. Teixeira, R.B. Caldas, L.F. Grilo, Influence of different shapes of geometric imperfections on the structural behavior of beams with large web openings, Adv. Steel Constr. 16 (2020) 272–278, https://doi.org/10.18057/IJASC.2020.16.3.8.
[12] D. Sonck, Global Buckling of Castellated and Cellular Steel Beams and Columns, PhD Thesis, Ghent University, 2014.
[13] D. Sonck, R. Van Impe, J. Belis, Experimental investigation of residual stresses in steel cellular and castellated members, Constr. Build. Mater. 54 (2014) 512–519, https://doi.org/10.1016/j.conbuildmat.2013.12.045.
[14] D. Sonck, J. Belis, Lateral–torsional buckling resistance of cellular beams, J. Constr. Steel Res. 105 (2015) 119–128, https://doi.org/10.1016/j.jcsr.2014.11.003.